

Search for dark matter annihilation in the center of the Earth with 8 years of IceCube data

Giovanni Renzi for the IceCube Collaboration
IIHE, Université Libre de Bruxelles

References

- [1] S. Sivertsson and J. Edsjö, Phys. Rev. D 85 (2012).
- [2] K. Griest and D. Seckel, Nucl. Phys. B 283 (1987) 681.
- [3] IceCube Collaboration, M. G. Aartsen et al., EPJ C 77 (2017) 82.
- [4] P. Mijakowski for Super-Kamiokande Collaboration 2020 J. Phys.: Conf. Ser. 1342 012075
- [5] ANTARES Collaboration, Phys. Dark Univ. 16 (2017) 41–48.

Dark matter from the center of the Earth

Dark Matter (DM) particles can scatter off nuclei in celestial bodies like Earth, lose energy, be **gravitationally captured** and **accumulate** in the center of the Earth.

This process of capture happens at a rate C_c that depends on the DM-nucleon spin-independent **scattering cross-section** σ_{SI} and the Earth chemical abundances.

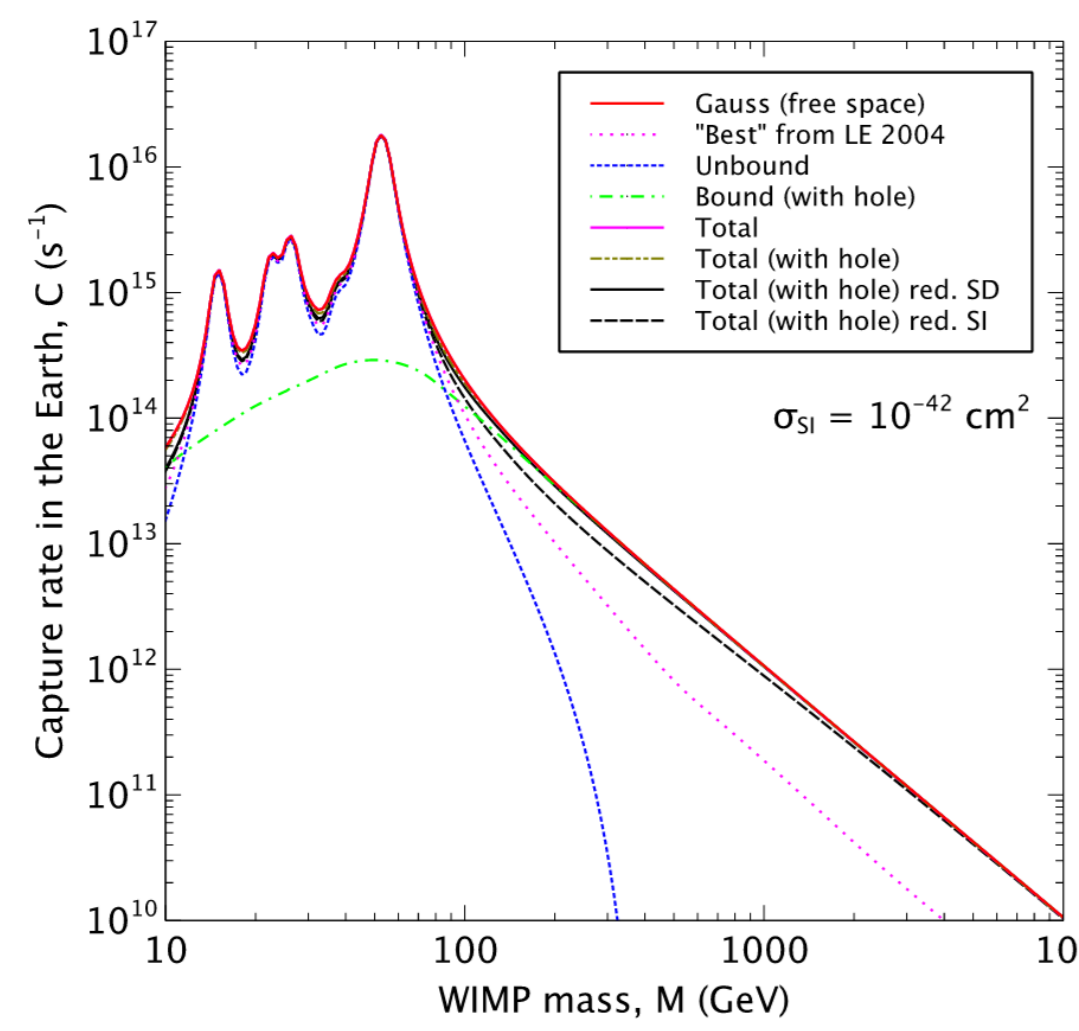
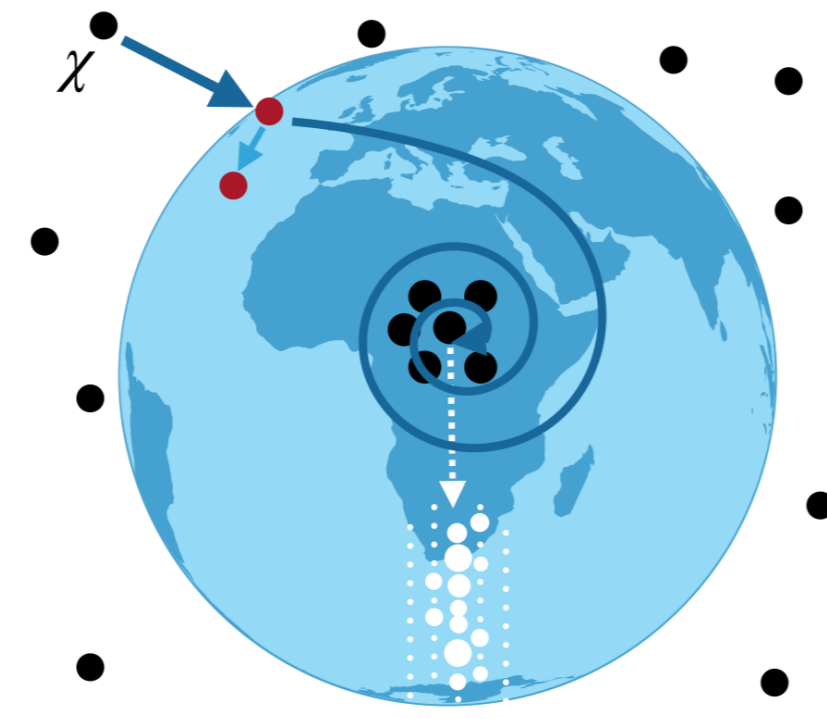


Fig. 1. Capture rate value vs. DM mass. From [1]



Accumulated DM particles can then **self-annihilate** into Standard Model particles.

The rate of the competing processes are related by:

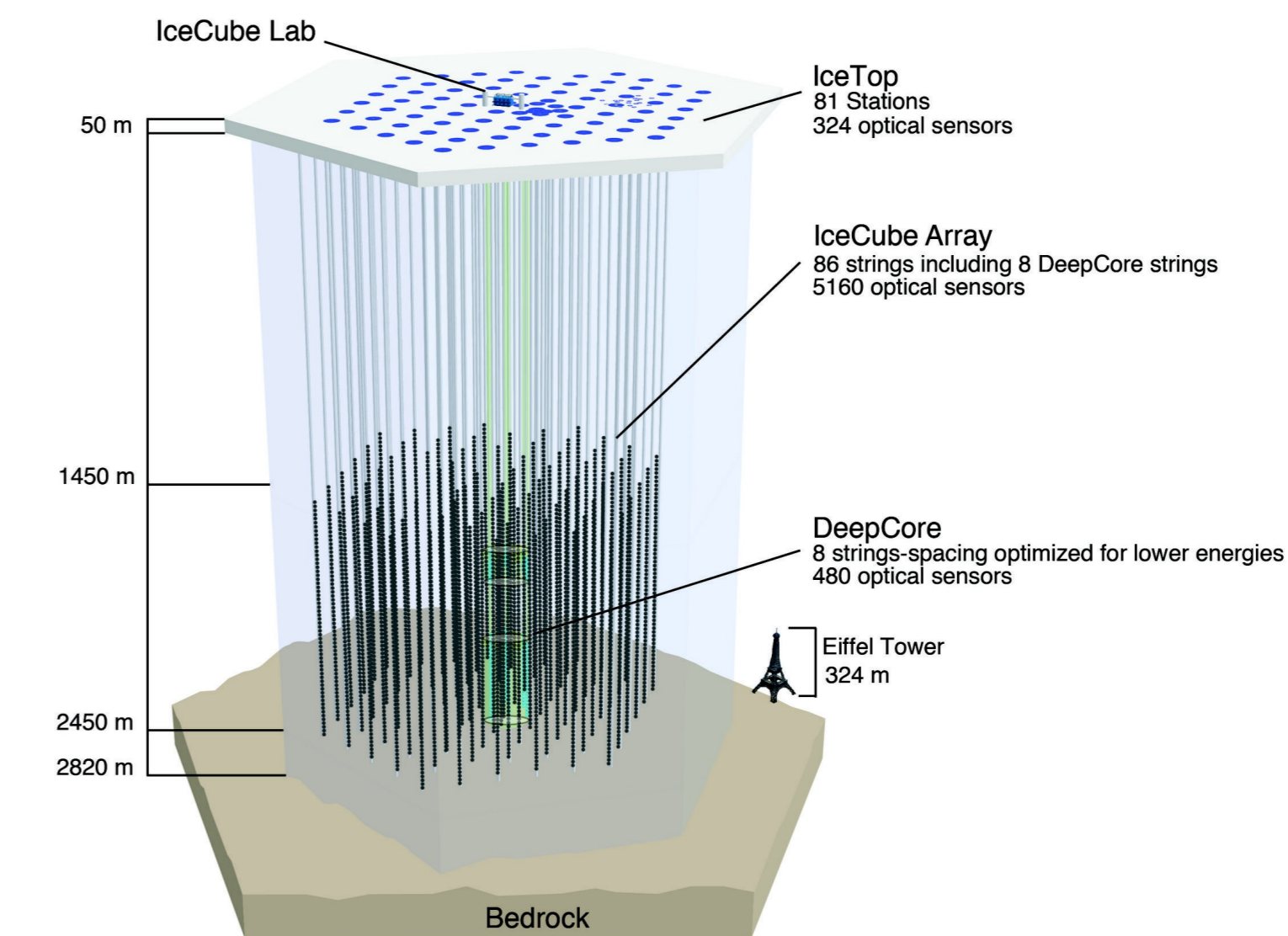
$$\frac{dN}{dt} = C_C - C_A N^2$$

where C_c is the **capture rate**. The second term describes annihilation, where the **annihilation rate** is defined as $\Gamma_A = \frac{1}{2} C_A N^2$ and is proportional to the **annihilation cross-section** $\langle \sigma_A v \rangle$. Given the Earth age, this process has not reached equilibrium yet.

The IceCube Neutrino Telescope

IceCube is a cubic kilometer neutrino detector located at the geographical South Pole and installed below 1450 m of ice.

An array of optical sensors collects the Cherenkov light emitted along the path of relativistic charged particles produced by neutrino interactions in the ice or bedrock.



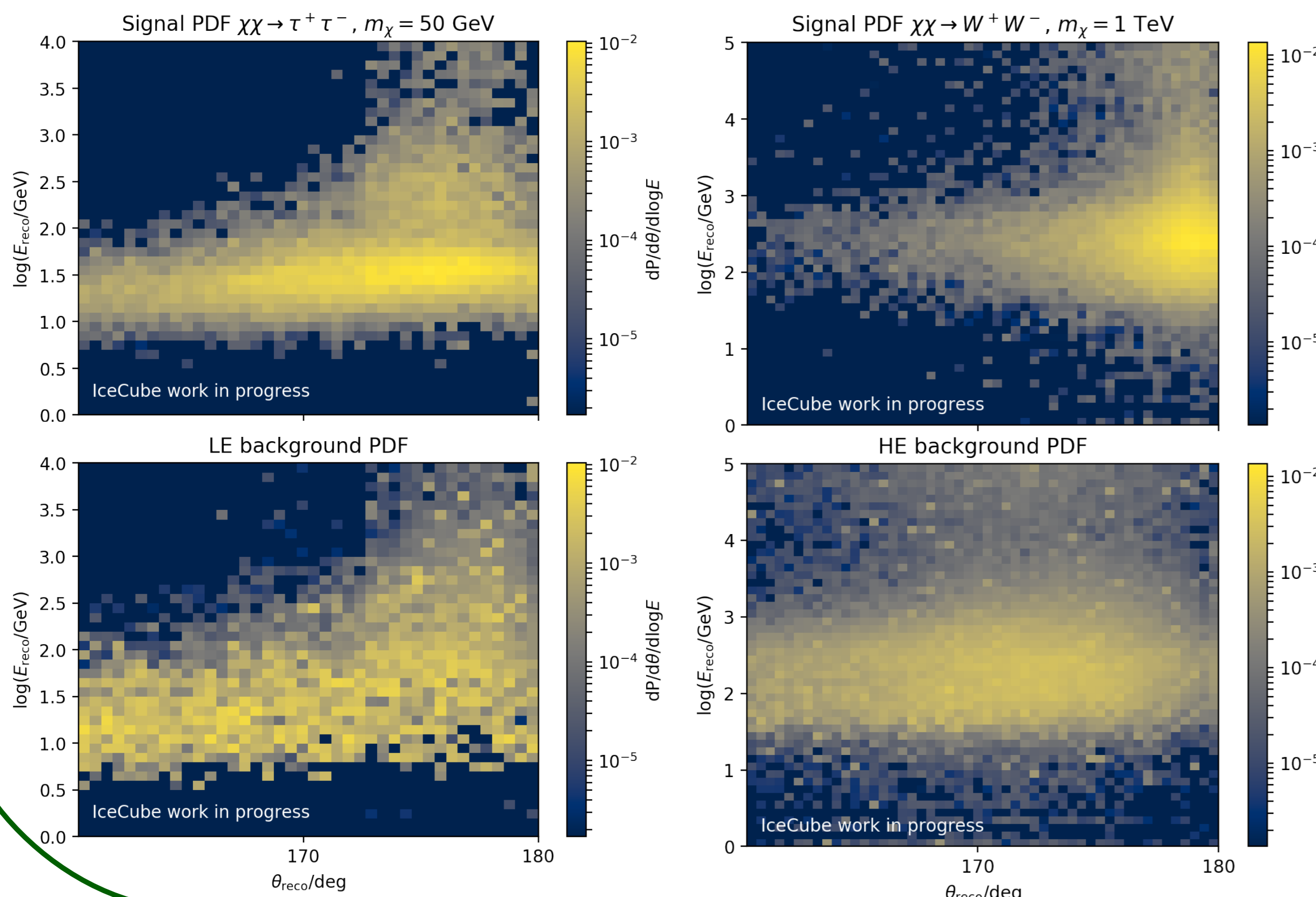
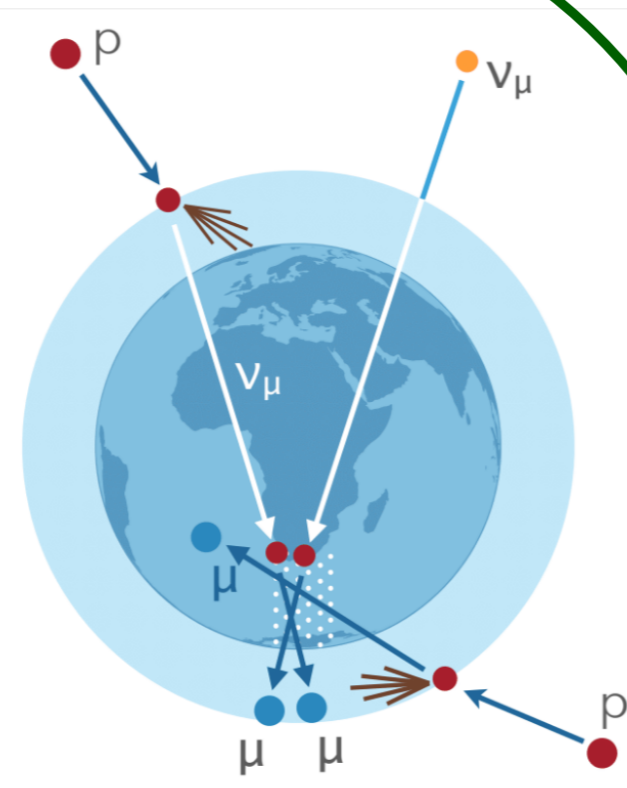
The pattern of the detected light signals makes it possible to reconstruct the characteristics of the particles passing through the volume of the detector, like for example the direction, the interaction vertex position and the energy.

Signal and background expectation

A DM annihilation **signal** will manifest as an excess of neutrinos coming from the center of the Earth at **zenith angles close to 180°**.

The **background** for this analysis consists of down-going mis-reconstructed **muons** and up-going **neutrinos** produced in cosmic rays air showers.

A dedicated **event selection** has been developed to discriminate signal from background. The event selection is split in low energy (LE) and high energy (HE) selections. This allows us to optimize the results on a wider range of masses.



The PDFs, shown in Fig. 2, are binned normalized distributions of reconstructed zenith angle vs. energy. The bin size is chosen in order to optimize the sensitivity results.

Fig. 2. PDFs for LE and HE reference signal and background.

Sensitivity

A binned likelihood test is performed, where the likelihood is defined as

$$\mathcal{L}(\mu) = \prod_{\text{bin}_i = \text{bin}_{\min}}^{\text{bin}_{\max}} \text{Poisson}(N_{\text{obs}}(\text{bin}_i) | N_{\text{obs}}^{\text{tot}} f(\text{bin}_i | \mu))$$

The function $f(\text{bin}_i | \mu)$ describes the probability function for a bin:

$$f(\text{bin}_i | \mu) = \mu S(\text{bin}_i) + (1 - \mu) B(\text{bin}_i)$$

where $S(\text{bin}_i)$ and $B(\text{bin}_i)$ are the PDFs for signal and background respectively (see Fig. 2) and μ is the fraction of signal.

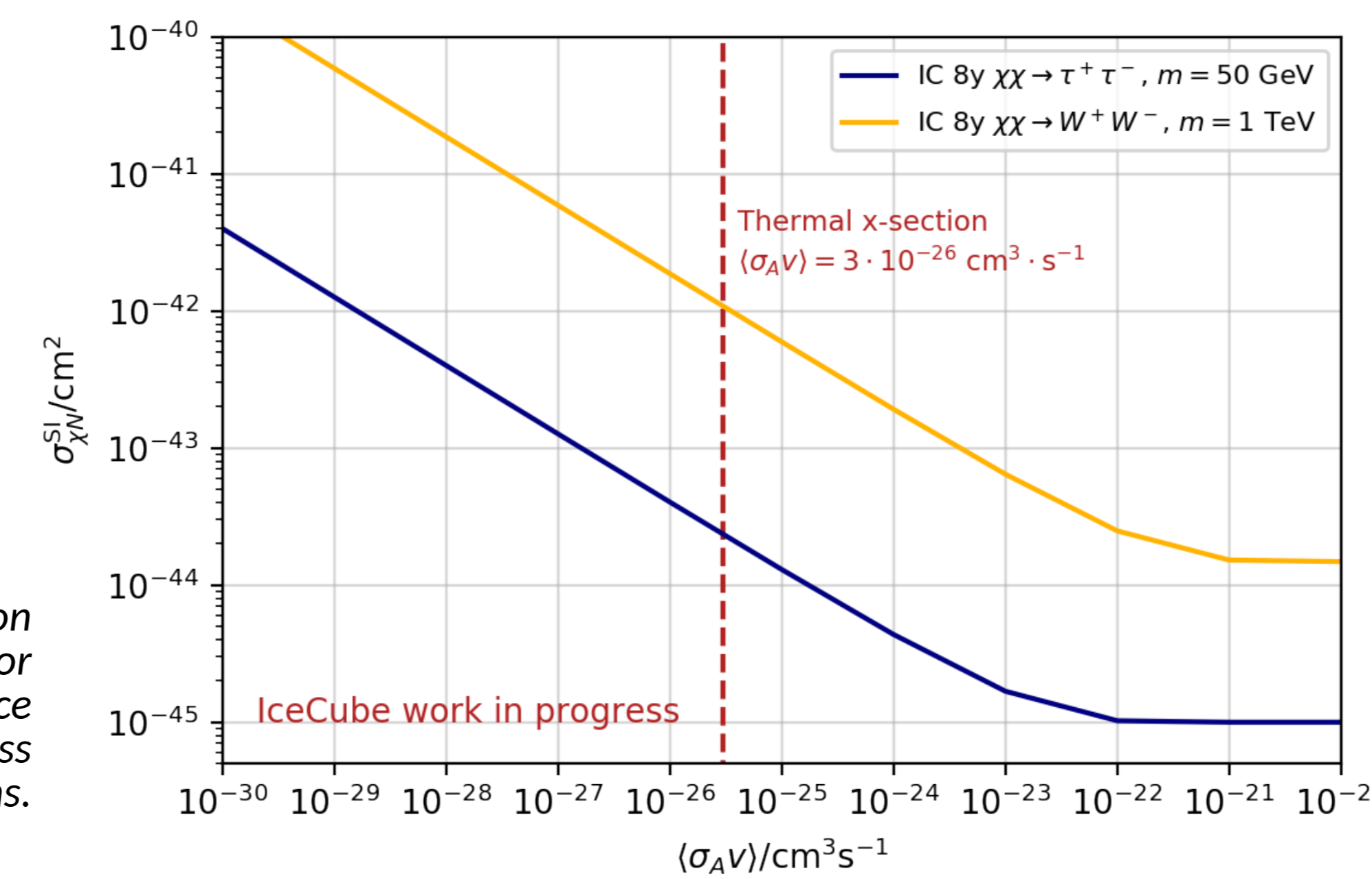


Fig. 3. Cross-section sensitivity scan for the two reference signal channel-mass combinations.

Spin Independent WIMP-nucleon cross section

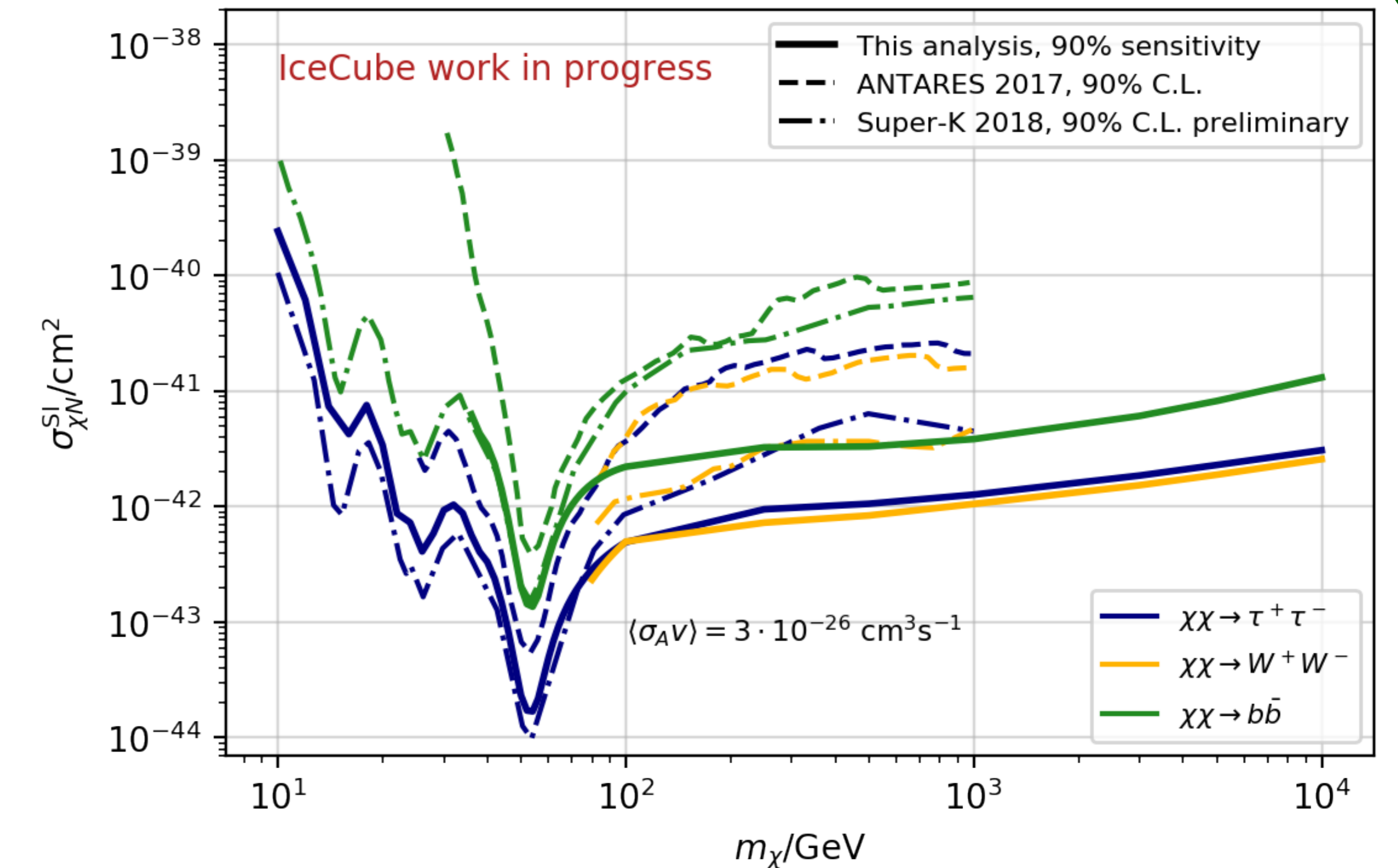


Fig. 4. Sensitivities at 90% C.L. for the spin-independent scattering cross-section σ_{SI} .

Given the non-equilibrium condition, to calculate the sensitivities on σ_{SI} , an assumption on $\langle \sigma_A v \rangle$ must be made. Fig. 3 shows the sensitivity on σ_{SI} for two masses and channels as a function of the $\langle \sigma_A v \rangle$ value assumed.

The **sensitivities** at the 90% C.L. on σ_{SI} are presented in Fig. 4. The results are compared to the current limits from Super-Kamiokande [4] and ANTARES [5].